Inorganic Chemistry
Article

Inorg. Chem. **2010**, *49*, 5943–5952 **5943**
DOI: 10.1021/ic100462r

A Series of New Phases Containing Three Different Asymmetric Building Units

Pei-Xin Li,[†,‡] Fang Kong,[†] Chun-Li Hu,[†] Na Zhao,[†,‡] and Jiang-Gao Mao*[,†]

[†]*State Key Laboratory of Structural Chemistry, Fujian Institute of Research on the Structure of Matter, Chinese Academy of Sciences, Fuzhou 350002, People's Republic of China, and* [‡]*Graduate School of the Chinese Academy of Sciences, Beijing 100039, People's Republic of China*

Received March 9, 2010

Systematic explorations of the new phases in the $Pb^{II}/Bi^{III}-TM(d^0/d^1)-Se^{IV}-O$ systems by hydrothermal syntheses led to five new quaternary phases whose structures are composed of three different asymmetric building units, namely, $Pb_2V^{V}{}_2Se_2O_{11}$ (**1**), $Pb_2V^{IV}{}_3Se_5O_{18}$ (**2**), $Pb_2Nb^{V}{}_2Se_4O_{15}$ (**3**), $Bi_2V^{V}{}_2Se_4O_{16}$ (**4**), and $Bi_2Mo^{VI}{}_2Se_2O_{13}$ (**5**). The structure of **1** features a 3D network built by 1D anionic chains of $[V_2O_5(SeO_3)_2]^{4-}$ interconnected by Pb^{2+} ions with six-membered-ring (MR) tunnels along the *b* axis. The structure of **2** features a 3D anionic framework composed of $V^{IV}O_6$ octahedra corner-sharing with SeO_3 anions, with the Pb^{2+} ions located at the resultant 8-MR tunnels. The oxidation state of the vanadium cation is 4+ due to the partial oxidation of V_2O_3 by SeO_2 at high temperature. The structure of **3** features novel 1D double chains of $[Nb_2O_3(SeO_3)_4]^{4-}$ that are interconnected by Pb^{2+} ions, forming a 3D network with 12-MR tunnels along the *c* axis. **4** features a 3D framework composed of 2D layers of $[Bi_2(SeO_3)_2]^{2+}$ and 1D $[(VO_2)_2(SeO_3)_2]^{2-}$ double chains. The structure of **5** features a 3D network composed of bismuth(III) selenite with large 10-MR tunnels along the *a* axis that are occupied by Mo_2O_{10} dimers. The results of optical diffuse-reflectance spectrum measurements and electronic structure calculations based on density functional theory methods indicate that all five compounds are wide-band-gap semiconductors. Luminescent property measurements for compounds **1**−**5** and magnetic measurements for compound **2** were also made.

Introduction

Open-framework and microporous inorganic materials have widespread applications in many fields such as catalysis, separation, and gas absorption.[1,2] Although such solids based on silicates, phosphates, germanates, borates, and phosphites have been extensively investigated, our knowledge about those based on the oxo anions of group 16 elements is still limited.[3,4] Recently, metal selenites and tellurites received increasing research attention from scientists in chemistry and materials. The presence of the lone pairs of Se^{IV} and Te^{IV} cations that are susceptible to the second-order Jahn−Teller (SOJT) distortions can serve as a structure-directing agent and aid in the formation of noncentrosymmetric (NCS) structures with possible second-harmonic generation (SHG).[5,6] Also, the combination of lone-pair cations with transition-metal ions with d^0 electronic configurations such as V^{5+}, Mo^{6+}, and Nb^{5+}, which are also susceptible to SOJT distortion, has proven to be an effective synthetic route for designing new promising SHG materials.[7] So far, alkali, alkaline-earth, or NH_4^+ ions are most often used as the countercations to balance the excess negative charges of the anionic architectures.[7] The post-transition-metal main-group IIIA cations such as Ga^{3+}/In^{3+} have also been used.[8] A number of lanthanide selenium(IV) and tellurium(IV) oxides with additional d^0 transition-metal ions

*To whom correspondence should be addressed. E-mail: mjg@fjirsm.ac.cn.

(1) Brinker, C. J. *Curr. Opin. Solid State Mater. Sci.* **1996**, *16*, 798–805.
(2) (a) Cheetham, A. K.; Ferey, G.; Loiseau, T. *Angew. Chem., Int. Ed.* **1999**, *38*, 3268. (b) Zhu, J.; Bu, X.; Feng, P.; Stucky, G. D. *J. Am. Chem. Soc.* **2000**, *122*, 11563.
(3) (a) Shen, Y.-L.; Jiang, H.-L.; Xu, J.; Mao, J.-G.; Cheah, K.-W. *Inorg. Chem.* **2005**, *44*, 9314–9321. (b) Millet, P.; Bastide, B.; Pashchenko, V.; Gnatchenko, S.; Gapon, V.; Ksari, Y.; Stepanov, A. *J. Mater. Chem.* **2001**, *11*, 1152–1157. (c) Effenberger, H. *Mineral. Petrol.* **1987**, *36*, 3–12. (d) Wildner, M. *J. Solid State Chem.* **1993**, *103*, 341–352.
(4) (a) Jiang, H.-L.; Kong, F.; Mao, J.-G. *J. Solid State Chem.* **2007**, *180*, 1764–1769. (b) Shen, Y. L.; Mao, J.-G. *Inorg. Chem.* **2005**, *44*, 5328–5335. (c) Harari, D.; Bernier, J. C.; Poix, P. *J. Solid State Chem.* **1972**, *5*, 382–390. (d) Harari, D.; Poix, P.; Bernier, J. D. *J. Solid State Chem.* **1974**, *11*, 330–339.
(5) (a) Wickleder, M. S. *Chem. Rev.* **2002**, *102*, 2011. (b) Verma, V. P. *Thermochim. Acta* **1999**, *327*, 63. (c) Ok, K. M.; Halasyamani, P. S. *Chem. Soc. Rev.* **2006**, *35*, 710.
(6) (a) Porter, Y.; Ok, K. M.; Bhuvanesh, N. S. P.; Halasyamani, P. S. *Chem. Mater.* **2001**, *13*, 1910. (b) Ok, K. M.; Bhuvanesh, N. S. P.; Halasyamani, P. S. *Inorg. Chem.* **2001**, *40*, 1978. (c) Kim, S. H.; Yeon, J.; Halasyamani, P. S. *Chem. Mater.* **2009**, *21*, 5335..
(7) (a) Halasyamani, P. S.; Poeppelmeier, K. R. *Chem. Mater.* **1998**, *10*, 2753. (b) Ra, H. S.; Ok, K. M.; Halasyamani, P. S. *J. Am. Chem. Soc.* **2003**, *125*, 7764. (c) Halasyamani, P. S. *Chem. Mater.* **2004**, *16*, 3586. (d) Ok, K. M.; Halasyamani, P. S. *Chem. Mater.* **2006**, *18*, 3176. (e) Chi, E. O.; Ok, K. M.; Porter, Y.; Halasyamani, P. S. *Chem. Mater.* **2006**, *18*, 2070. (f) Hart, R. T.; Ok, K. M.; Halasyamani, P. S.; Zwanziger, J. W. *Appl. Phys. Lett.* **2004**, *85*, 938. (g) Goodey, J.; Broussard, J.; Halasyamani, P. S. *Chem. Mater.* **2002**, *14*, 3174. (h) Johnston, M. G.; Harrison, W. T. A. *Inorg. Chem.* **2001**, *40*, 6518. (i) Balraj, V.; Vidyasagar, K. *Inorg. Chem.* **1999**, *38*, 5809.
(8) Kong, F.; Hu, Ch.-L.; Hu, T.; Zhou, Y.; Mao, J.-G. *J. Chem. Soc., Dalton Trans.* **2009**, 4962.

Published on Web 06/07/2010

have also been reported mainly by our group.[9] Because of the higher coordination numbers for the lanthanide ions, the corresponding lanthanide(III) compounds containing both types of SOJT distortion cations are usually structurally centrosymmetric and therefore not SHG-active. However, they can exhibit strong luminescence in the visible or near-IR region.[9] Furthermore, a few compounds of the transition metal (TM)−d^0/d^1 TM−Se^{IV}/Te^{IV}−O systems have also been reported.[10]

The Pb^{II} and Bi^{III} cations also have a lone pair that is normally less stereochemically active than the selenite or tellurite anions.[11] It would be interesting to explore the new phases in the Pb^{2+}/Bi^{3+}−d^0 TM−Se^{IV}/Te^{IV}−O systems to verify if the combination of three different asymmetric units in the same compound can help the formation of the NCS structures. Up to now, only several such tellurites have been reported, but no such selenites has been found to the best of our knowledge.[12] $Bi_2Te_2WO_{10}$ features one-dimensional (1D) chains of $[WO_4(TeO_3)_2]^{4-}$ anions interconnected by Bi^{3+} ions, and $Bi_2Te_2W_3O_{16}$ features triple-decker chains of $[W_3O_{10}(TeO_3)_2]^{4-}$ interconnected by Bi^{3+} ions.[12a,b] $BiNbTe_2O_8$ can be described as layers of corner-shared NbO_6 octahedra and fluorite-like sheets of BiO_8 distorted cubes and $Te1O_4$ disphenoids interconnected by $Te2O_3$ pyramids via Nb−O4−Te2−O8−Bi bridges.[12d] $Pb_4Te_6M_{10}O_{41}$ (M = Nb^{5+} or Ta^{5+}) exhibits a three-dimensional (3D) framework consisting of layers of corner-shared NbO_6 octahedra connected by TeO_3 and PbO_6 polyhedra.[12e] It has been demonstrated that the selenites normally display structures different from those of corresponding tellurites owing to the fact that Te^{IV} can be three-, four-, or five-coordinated and these $Te^{IV}O_x$ (x = 3−5)[13] polyhedra may polymerize into various isolated clusters or extended structures, whereas only SeO_3^{2-} or $Se_2O_5^{2-}$ are reported for the metal selenites. Hence, a variety of new compounds with novel structures and physical properties may be formed in the Pb^{II}/Bi^{III}−TM(d^0)−Se^{IV}−O systems. Our research efforts in this aspect led to five new compounds with five different structural types, namely, $Pb_2V^V{}_2Se_2O_{11}$ (**1**) and $Pb_2V^{IV}{}_3Se_5O_{18}$ (**2**), in which the vanadium cation is in the d^1 electronic configuaration, and $Pb_2Nb^V{}_2Se_4O_{15}$ (**3**), $Bi_2V^V{}_2Se_4O_{16}$ (**4**), and $Bi_2Mo^{VI}{}_2Se_2O_{13}$ (**5**). Herein, we report their syntheses and crystal and band structures as well as their optical properties.

Experimental Section

Materials and Instrumentation. All of the chemicals were analytically pure from commercial sources and used without further purification. Microprobe elemental analyses for Pb, V, Nb, Mo, and Se were performed with a JEOL-6700F scanning electron microscope. Powder X-ray diffraction (XRD) patterns (Cu Kα) were collected on an XPERT-MPD $\theta-2\theta$ diffractometer. IR spectra were recorded on a Magna 750 FT-IR spectrometer as KBr pellets in the range of 4000−400 cm^{-1}. Thermogravimetric analyses (TGA) were carried out with a NETZSCH STA 449C unit, at a heating rate of 10 °C/min under a nitrogen atmosphere. Photoluminescence analyses were performed with an Edinburgh FLS920 fluorescence spectrometer. Optical diffuse-reflectance spectra were measured at room temperature with a PE Lambda 900 UV−visible spectrophotometer. The instrument was equipped with an integrating sphere and controlled by a personal computer. A $BaSO_4$ plate was used as the standard (100% reflectance). The absorption spectra were calculated from a reflectance spectrum using the Kubelka−Munk function: $\alpha/S = (1-R)^2/2R$,[14] where α is the absorption coefficient, S is the scattering coefficient, which is practically wavelength-independent when the particle size is larger than 5 μm, and R is the reflectance. Magnetic susceptibility measurements for compound **2** were performed with a PPMS-9T magnetometer at 1000 Oe in the temperature range of 2−300 K. The raw data were corrected for the susceptibility of the container and the diamagnetic contributions of the sample using Pascal constants.[15]

Synthesis of Compounds 1−5. The five compounds were hydrothermally synthesized by reactions of a mixture of PbO (or Bi_2O_3), V_2O_3 (or Nb_2O_5 or MoO_3), and SeO_2 in 5−8 mL of distilled water, at 200 or 230 °C for 4−5 days.

The loaded compositions are as follows: PbO (0.0663 g, 0.30 mmol), V_2O_3 (0.0226 g, 0.15 mmol), SeO_2 (0.1130 g, 1.02 mmol), and H_2O (5.0 mL) for $Pb_2V^V{}_2Se_2O_{11}$ (**1**); PbO (0.0662 g, 0.30 mmol), V_2O_3 (0.0225 g, 0.15 mmol), SeO_2 (0.1264 g, 1.10 mmol), and H_2O (5.0 mL) for $Pb_2V^{IV}{}_3Se_5O_{18}$ (**2**); PbO (0.0361 g, 0.16 mmol), Nb_2O_5 (0.0415 g, 0.16 mmol), SeO_2 (0.1181 g, 0.51 mmol), and H_2O (8.0 mL) for $Pb_2Nb^V{}_2Se_4O_{15}$ (**3**); Bi_2O_3 (0.0469 g, 0.10 mmol), V_2O_3 (0.0294 g, 0.20 mmol), SeO_2 (0.1111 g, 1.00 mmol), and H_2O (8.0 mL) for $Bi_2V^V{}_2Se_4O_{12}$ (**4**); Bi_2O_3 (0.2330 g, 0.50 mmol), MoO_3 (0.1440 g, 1 mmol), SeO_2 (0.1660 g, 1.50 mmol), and H_2O (6.0 mL) for $Bi_2Mo^{VI}{}_2Se_2O_{13}$ (**5**). The initial and final pH values of the reaction media are close to 2.0 for all five compounds. The excess SeO_2 aided in the crystallization of the five compounds because of its high solubility in water. The reagent of V_2O_3 has been oxidized for the higher value states: 5+ (at 200 °C for **1** and **4**) or 4+ (at 230 °C for **2**), probably by oxidization of SeO_2. When V_2O_5 was used instead of V_2O_3, compounds **1**, **2**, and **4** could not be obtained. Single crystals of **1**, **2**, and **4** were collected in a very low yield (< 30.0 mg) because of the incomplete redox reaction. For the synthesis of compound **1**, the byproducts are yellow powders and a few unknown yellow rectangular crystals with very poor crystal quantity. For the synthesis of compound **2**, the only byproduct is a dark-gray powder, and in the case of compound **4**, it is a yellow powder. Single crystals of **1**, **2**, and **4**, selected based on their unique shapes and colors, were used for their IR, UV, and magnetic measurements. Single crystals of **3** were collected in a yield of 51% (based on Pb) and single crystals of **5** were collected in a yield of 60% yield (based on Bi) as single phases. Their purities were confirmed by powder XRD studies.

The results of microprobe elemental analyses on several single crystals of compounds **1**−**5** gave an average molar ratio of Pb/V/Se of 1.0/1.0/1.1 for **1**, Pb/V/Se of 1.0/1.5/2.6 for **2**, Pb/Nb/Se

(9) (a) Shen, Y.-L.; Jiang, H.-L.; Xu, J.; Mao, J.-G.; Cheah, K. W. *Inorg. Chem.* **2005**, *44*, 9314. (b) Jiang, H.-L.; Ma, E.; Mao, J.-G. *Inorg. Chem.* **2007**, *46*, 7012.

(10) (a) Jiang, H.-L.; Xie, Z.; Mao, J.-G. *Inorg. Chem.* **2007**, *46*, 6495. (b) Jiang, H.-L.; Huang, Sh.-P.; Fan, Y.; Mao, J.-G.; Chen, W.-D. *Chem.—Eur. J.* **2008**, *14*, 1972. (c) Jiang, H.-L.; Kong, F.; Fan, Y.; Mao, J.-G. *Inorg. Chem.* **2008**, *47*, 7430. (d) Mao, J.-G.; Jiang, H.-L.; Kong, F. *Inorg. Chem.* **2008**, *47*, 8498. (e) Zhang, S.-Y.; Jiang, H.-L.; Sun, C.-F.; Mao, J.-G. *Inorg. Chem.* **2009**, *48*, 11809.

(11) Zhang, W.-L.; Lin, X.-S.; Zhang, H.; Wang, J.-Y.; Lin, Ch.-Sh.; He, Z.-Z.; Cheng, W.-D. *J. Chem. Soc., Dalton Trans.* **2010**, *39*, 1546.

(12) (a) Champarnaud-Mesjard, J. C.; Frit, B.; Chagraoui, A.; Tairi, A. *Z. Anorg. Allg. Chem.* **1996**, *622*, 1907. (b) Champarnaud-Mesjard, J. C.; Frit, B.; Chagraoui, A.; Tairi, A. *J. Solid State Chem.* **1996**, *127*, 248. (c) Castro, A.; Enjalbert, R.; Baules, P.; Galy, J. *J. Solid State Chem.* **1998**, *139*, 185. (d) Blanchandin, S.; Champarnaud-Mesjard, J. C.; Thomas, P.; Frit, B. *Solid State Sci.* **2000**, *2*, 223. (e) Ok, K. M.; Halasyamani, P. S. *Inorg. Chem.* **2004**, *43*, 4248.

(13) (a) Jiang, H.-L.; Mao, J.-G. *Inorg. Chem.* **2006**, *45*, 717–721. (b) Nikiforov, G. B.; Kusainova, A. M.; Berdonosov, P. S.; Dolgikh, V. A.; Lightfoot, P. *J. Solid State Chem.* **1999**, *146*, 473. (c) Meier, S. F.; Schleid, T. *Z. Anorg. Allg. Chem.* **2003**, *629*, 1575.

(14) Wendlandt, W. M.; Hecht, H. G. *Reflectance Spectroscopy*; Interscience: New York, 1966.

(15) Kahn, O. *Molecular Magnetism*; VCH Publishers, Inc.: New York, 1993.

Table 1. Summary of the Crystal Data and Structural Refinement Parameters for **1**−**5**

	1	**2**	**3**	**4**	**5**
formula	$Pb_2V^V{}_2Se_2O_{11}$	$Pb_2V^{IV}{}_3Se_5O_{18}$	$Pb_2Nb^V{}_2Se_4O_{15}$	$Bi_2V^V{}_2Se_4O_{16}$	$Bi_2Mo^{VI}{}_2Se_2O_{13}$
fw	850.18	1250.00	1156.04	1091.68	975.76
space group	$P\bar{1}$ (No. 2)	*Pnma* (No. 62)	*C*2/*c* (No. 15)	*P*2(1)/*c* (No. 14)	$P\bar{1}$ (No. 2)
a, Å	6.832(3)	17.013(3)	26.49(1)	6.782(2)	6.585(7)
b, Å	7.181(3)	10.710(2)	7.001(3)	7.176(2)	6.929(9)
c, Å	9.857(5)	9.059(1)	7.686(3)	27.047(8)	11.62(1)
α, deg	96.031(4)	90	90	90	89.76(4)
β, deg	93.657(6)	90	94.503(7)	90.300(4)	82.45(3)
γ, deg	95.455(7)	90	90	90	86.40(4)
V, Å^3	477.4(4)	1650.6(4)	1421(1)	1316.4(6)	525(1)
Z	2	4	4	4	2
D_{calcd}, g/cm^3	5.914	5.030	5.403	5.508	6.179
μ, mm^{-1}	44.732	33.088	35.517	39.187	42.803
GOF on F^2	1.035	1.053	1.086	1.013	0.996
R1, wR2 [$I > 2\sigma(I)$][a]	0.0256, 0.0620	0.0198, 0.0471	0.0359, 0.0811	0.0308, 0.0598	0.0205, 0.0382
R1, wR2 (all data)	0.0295, 0.0631	0.0222, 0.0478	0.0422, 0.0834	0.0439, 0.0646	0.0275, 0.0407

[a] $R1 = \sum||F_o| - |F_c||/\sum|F_o|$; $wR2 = \{\sum w[(F_o)^2 - (F_c)^2]^2/\sum w[(F_o)^2]^2\}^{1/2}$.

of 1.0/1.2/1.9 for **3**, Bi/V/Se of 1.0/1.0/1.8 for **4**, and Bi/Mo/Se of 1.0/1.1/1.1 for **5**, respectively, which are in good agreement with the ones determined from single-crystal X-ray structural analyses. IR data (KBr, cm^{-1}) for **1**: 910 m, 886 m, 820 s, 784 s, 714 m, 684 m, 661 m, 607 m, 555 m, 516 w, 500 w, 439 w. IR data (KBr, cm^{-1}) for **2**: 985 m, 970 m, 950 w, 897 w, 811 m, 754 s, 711 vs, 665 s, 575 m, 535 m, 510 m, 480 w, 432 w. IR data (KBr, cm^{-1}) for **3**: 937 m, 853 s, 747 vs, 722 vs, 620 s, 506 m, 482 w, 447 w, 424 w. IR data (KBr, cm^{-1}) for **4**: 920 m, 870 m, 856 m, 786 s, 702 m, 667 m, 642 m, 591 m, 512 m, 486 m, 427 w. IR data (KBr, cm^{-1}) for **5**: 925 m, 860 s, 752 s, 665 s, 565 m, 501 m, 449 w. The measured powder XRD patterns for all five compounds are in agreement with the simulated ones from their single-crystal data (Figure S1 in the Supporting Information).

Single-Crystal Structure Determination. Data collections for the five compounds were performed on a SATURN 70 CCD diffractometer equipped with graphite-monochromated Mo Kα radiation (λ = 0.710 73 Å) at 293(2) K. The date sets were corrected for Lorentz and polarization factors as well as for absorption by a Multiscan method.[16a] All five structures were solved by direct methods and refined by full-matrix least-squares fitting on F^2 by *SHELX-97*.[16b] All of the non-H atoms were refined with anisotropic thermal parameters. Crystallographic data and structural refinements for the five compounds are summarized in Table 1. Important bond distances are listed in Table 2. More details on the crystallographic studies as well as atomic displacement parameters are given as Supporting Information.

Computational Descriptions. Single-crystal structural data of the five compounds were used for the theoretical calculations. The ab initio band structure calculations and density of states (DOS) were performed by using the computer code CASTEP.[17] The code employs density functional theory (DFT) using a plane-wave basis set with Vanderbilt norm-conserving pseudopotentials to approximate the interactions between the core and valence electrons.[18] The exchange-correlation energy was calculated using the Perdew−Burke−Ernzerh of modification to the generalized gradient approximation (GGA).[19] The number of plane waves included in the basis set is determined by a kinetic-energy cutoff of

Table 2. Selected Bond Lengths (Å) for Compounds **1**−**5**[a]

	Compound **1**		
Pb1−O5#1	2.449(5)	Pb1−O9#2	2.508(4)
Pb1−O3#3	2.518(5)	Pb1−O8#4	2.575(5)
Pb1−O2	2.622(5)	Pb2−O2#5	2.364(5)
Pb2−O9#2	2.452(5)	Pb2−O1	2.586(5)
Pb2−O10	2.638(5)	Pb2−O4	2.760(5)
V1−O7	1.626(5)	V1−O8	1.716(5)
V1−O11#6	1.877(4)	V1−O6	1.995(5)
V1−O4#7	2.171(5)	V1−O11	2.302(5)
V2−O10	1.638(4)	V2−O9	1.680(5)
V2−O11	1.861(4)	V2−O3#8	1.981(5)
V2−O8	2.114(5)	V2−O4#9	2.347(4)
Se1−O1	1.690(5)	Se1−O2	1.714(5)
Se1−O3	1.743(5)	Se2−O5	1.673(5)
Se2−O4	1.719(5)	Se2−O6	1.727(5)
	Compound **2**		
Pb1−O5#1	2.474(3)	Pb1−O5#2	2.474(3)
Pb1−O4	2.605(3)	Pb1−O4#3	2.605(3)
Pb1−O8	2.646(3)	Pb1−O8#3	2.646(3)
Pb2−O3	2.552(3)	Pb2−O3#4	2.552(3)
Pb2−O6#4	2.590(3)	Pb2−O6	2.590(3)
V1−O9	1.595(4)	V1−O7#5	2.030(3)
V1−O7#6	2.030(3)	V1−O8	2.057(3)
V1−O8#3	2.057(3)	V1−O1	2.089(5)
V2−O10	1.590(3)	V2−O2#7	1.958(3)
V2−O3#8	2.001(3)	V2−O6	2.047(3)
V2−O4	2.100(3)	V2−O5	2.256(3)
Se1−O1	1.640(5)	Se1−O2	1.711(3)
Se1−O2#3	1.711(3)	Se2−O5	1.686(3)
Se2−O3	1.715(3)	Se2−O4	1.728(3)
Se3−O6	1.704(3)	Se3−O8	1.704(3)
Se3−O7	1.715(3)		
	Compound **3**		
Pb1−O2#1	2.393(8)	Pb1−O1#2	2.451(8)
Pb1−O5#3	2.549(8)	Pb1−O2#4	2.629(8)
Pb1−O1#5	2.639(8)	Nb1−O7	1.776(7)
Nb1−O8	1.8924(13)	Nb1−O6	2.005(8)
Nb1−O4#4	2.036(7)	Nb1−O3	2.055(8)
Nb1−O7#4	2.207(7)	Se1−O1	1.677(7)
Se1−O2	1.702(8)	Se1−O3	1.725(8)
Se2−O5	1.653(8)	Se2−O4	1.712(7)
Se2−O6	1.730(7)		
	Compound **4**		
Bi1−O9	2.204(6)	Bi1−O5#1	2.407(5)
Bi1−O1	2.410(5)	Bi1−O2	2.416(6)

(16) (a) *CrystalClear*, version 1.3.5; Rigaku Corp.: The Woodlands, TX, 1999. (b) Sheldrick, G. M. *SHELXTL, Crystallographic Software Package*, version 5.1; Bruker-AXS: Madison, WI, 1998.

(17) (a) Segall, M. D.; Lindan, P. J. D.; Probert, M. J.; Pickard, C. J.; Hasnip, P. J.; Clark, S. J.; Payne, M. C. *J. Phys.: Condens. Matter* **2002**, *14*, 2717. (b) Milman, V.; Winkler, B.; White, J. A.; Pickard, C. J.; Payne, M. C.; Akhmatskaya, E. V.; Nobes, R. H. *Int. J. Quantum Chem.* **2000**, *77*, 895.

(18) Lin, J. S.; Qteish, A.; Payne, M. C.; Heine, V. *Phys. Rev. B* **1993**, *47*, 4174.

(19) Perdew, J. P.; Burke, K.; Ernzerhof, M. *Phys. Rev. Lett.* **1996**, *77*, 3865.

Table 2. Continued

Compound **4**			
Bi1−O6#2	2.426(5)	Bi1−O3#3	2.639(6)
Bi1−O4	2.705(6)	Bi2−O4#4	2.242(6)
Bi2−O2#5	2.368(5)	Bi2−O12#6	2.404(5)
Bi2−O1	2.415(5)	Bi2−O3#4	2.426(6)
Bi2−O13#6	2.622(6)	Bi2−O6#1	2.715(6)
V1−O15	1.633(6)	V1−O14	1.666(5)
V1−O7	1.947(5)	V1−O10	1.982(5)
V1−O16#7	2.165(5)	V1−O10#8	2.347(6)
V2−O13	1.639(5)	V2−O16	1.663(5)
V2−O8#5	1.964(6)	V2−O11	1.977(5)
V2−O14	2.127(5)	V2−O11#9	2.323(6)
Se1−O3	1.698(5)	Se1−O2	1.715(5)
Se1−O1	1.719(5)	Se2−O5	1.696(5)
Se2−O4	1.699(6)	Se2−O6	1.706(5)
Se3−O9	1.686(6)	Se3−O7	1.707(5)
Se3−O8	1.707(5)	Se4−O12	1.655(5)
Se4−O11	1.748(5)	Se4−O10	1.750(5)
Compound **5**			
Bi1−O8	2.331(5)	Bi1−O8#1	2.342(5)
Bi1−O9	2.367(4)	Bi1−O5	2.455(5)
Bi1−O3	2.464(6)	Bi1−O7	2.485(5)
Bi1−O6	2.580(5)	Bi2−O12	2.253(4)
Bi2−O13	2.253(5)	Bi2−O4#2	2.323(5)
Bi2−O1#3	2.390(5)	Bi2−O2	2.545(5)
Bi2−O3#4	2.644(5)	Bi2−O1#4	2.678(5)
Mo1−O10	1.711(5)	Mo1−O6#4	1.713(5)
Mo1−O8	1.933(4)	Mo1−O12#5	1.948(4)
Mo1−O5#1	2.230(5)	Mo1−O9	2.255(5)
Mo2−O11	1.713(5)	Mo2−O13#6	1.745(4)
Mo2−O9#7	1.811(4)	Mo2−O2	2.056(4)
Mo2−O12	2.103(5)	Mo2−O7	2.444(5)
Se1−O3	1.677(5)	Se1−O1	1.690(5)
Se1−O2	1.748(4)	Se2−O4	1.695(4)
Se2−O5	1.726(5)	Se2−O7#2	1.730(5)

[a] Symmetry transformations used to generate equivalent atoms. For **1**: #1, $x+1, y, z$; #2, $x, y-1, z$; #3, $-x+1, -y+1, -z+2$; #4, $x+1, y-1, z$; #5, $-x, -y+1, -z+2$; #6, $-x-1, -y+2, -z+1$; #7, $-x-1, -y+1, -z+1$; #8, $-x, -y+2, -z+2$; #9, $x, y+1, z$. For **2**: #1, $-x-{}^1/_2, +y-{}^1/_2, z-{}^1/_2$; #2, $-x-{}^1/_2, -y, z-{}^1/_2$; #3, $x, -y-{}^1/_2, z$; #4, $x, -y+{}^1/_2, z$; #5, $-x, -y, -z+2$; #6, $-x, y-{}^1/_2, -z+2$; #7, $-x, -y, -z+3$; #8, $-x-{}^1/_2, -y, z+{}^1/_2$. For **3**: #1, $-x+{}^1/_2, y-{}^1/_2, -z+{}^1/_2$; #2, $x, -y, z-{}^1/_2$; #3, $x, y, z-1$; #4, $x, -y+1, z-{}^1/_2$; #5, $-x+{}^1/_2, -y+{}^1/_2, -z+1$. For **4**: #1, $-x+1, y-{}^1/_2, -z+{}^1/_2$; #2, $-x+1, y+{}^1/_2, -z+{}^1/_2$; #3, $x+1, y, z$; #4, $-x, y-{}^1/_2, -z+{}^1/_2$; #5, $x, y-1, z$; #6, $x-1, y, z$; #7, $x, y+1, z$; #8, $-x+2, -y, -z$; #9, $-x+2, -y-1, -z$; #10, $-x, y+{}^1/_2, -z+{}^1/_2$. For **5**: #1, $-x+2, -y, -z$; #2, $-x+2, -y+1, -z$; #3, $-x+2, -y+1, -z+1$; #4, $x+1, y, z$; #5, $x, y-1, z$; #6, $x-1, y, z$; #7, $x, y+1, z$.

700 eV for **1**−**4** and 500 eV for **5**. The numerical integration of the Brillouin zone is performed by using $4\times4\times3$, $1\times2\times3$, $4\times4\times3$, $4\times3\times1$, and $4\times4\times2$ Monkhorst−Pack k-point sampling for **1**−**5**, respectively. Pseudoatomic calculations were performed for O $2s^2 2p^4$, Se $4s^2 4p^4$, V $3d^3 4s^2$, Mo $3d^4 4s^2$, Pb $5d^{10} 6s^2 6p^2$, Bi $5d^{10} 6s^2 6p^3$, and Nb $4d^4 5s^1$. Spin polarization was included for the electronic structure calculations of **2**. The other calculating parameters used in the calculations and convergent criteria were set by the default values of the CASTEP code.

Results and Discussion

Structural Descriptions. The reactions of PbO (or Bi_2O_3) with a lone pair, V_2O_3 (or Nb_2O_5 or MoO_3), and SeO_2 afforded five novel selenites with different structures, namely, $Pb_2V^V{}_2Se_2O_{11}$ (**1**), $Pb_2V^{IV}{}_3Se_5O_{18}$ (**2**), $Pb_2Nb^V{}_2Se_4O_{15}$ (**3**), $Bi_2V^V{}_2Se_4O_{16}$ (**4**), and $Bi_2Mo^{VI}{}_2Se_2O_{13}$ (**5**). These compounds represent the first examples of Pb^{II} or Bi^{III} d^0/d^1 transition-metal selenites. All five

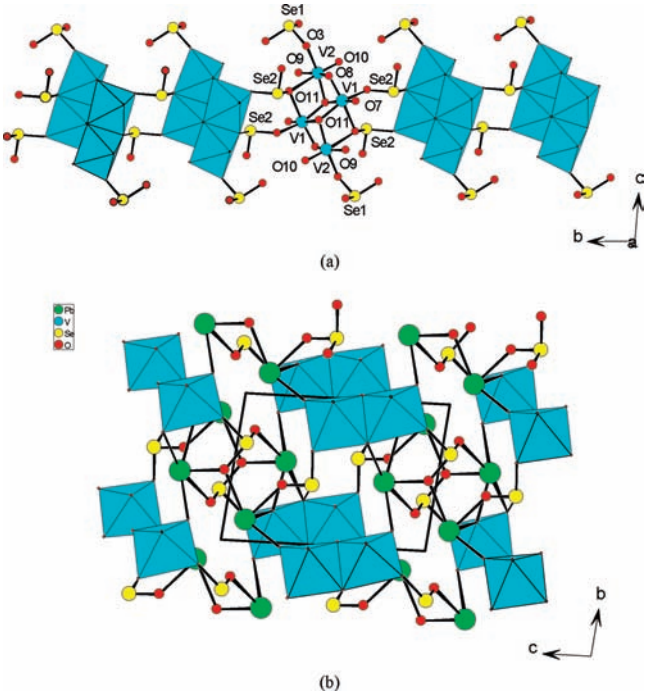

Figure 1. 1D chain of $[V_2O_5(SeO_3)_2]^{4-}$ anions (a) and view of the structure of **1** along the a axis (b). VO_6 octahedra are shaded in cyan. Pb, Se, and O atoms are represented by green, yellow, and red circles, respectively.

compounds contain three different asymmetric building blocks: two different cations with a lone pair and a distorted MO_6 (M = V, Nb, Mo) octahedron. Their structures belong to five different types. It is interesting to note that three vanadium phases were formed through oxidation of the V^{3+} ion. These compounds cannot be prepared using V_2O_5 as the vanadium source. The chemistry of vanadate ions in aqueous solution is well established, and a variety of vanadate ions can be obtained by controlling the pH, concentration, reaction time, and temperature.[20]

The structure of **1** features 1D $[V_2O_5(SeO_3)_2]^{4-}$ chains that are further bridged by Pb^{2+} cations in a 3D network (Figure 1). There are two Pb^{II} atoms, two V^{5+} cations, five oxo anions, and two selenite anions in the asymmetric unit of **1**; hence, **1** can also be formulated as $Pb_2V^V{}_2O_5(SeO_3)_2$.

When only the normal Pb−O bonds are considered, both Pb^{II} ions are five-coordinated by three selenite anions in a unidentate fashion and two O^{2-} anions (Scheme S1a,b in the Supporting Information). The Pb−O distances range from 2.364(5) to 2.760(5) Å. The five O atoms are on the same side of the Pb^{2+} cation, confirming the presence of a stereochemically active lone pair of each Pb^{2+} cation. Both V1 and V2 are six-coordinated by two selenite anions in a unidentate fashion and four O^{2-} anions in a severely distorted octahedral geometry. The V−O distances range from 1.626(5) to 2.302(5) Å and from 1.638(4) to 2.347(5) Å for V1 and V2, respectively. The O−V−O bond angles fall in the range of 77.48(19)−174.6(2)°. Taking into account the six V−O bond lengths as well as the deviations from 180° of

(20) (a) Berrocal, T.; Mesa, J. L.; Pizarro, J. L.; Bazan, B.; Iglesias, M.; Vilas, J. L.; Rojoa, T.; Arriortua, M. I. *Dalton Trans.* **2010**, *39*, 834. (b) Aldous, D. W.; Goff, R. J.; Attfield, J. P.; Lightfoot, P. *Inorg. Chem.* **2007**, *46*, 1277.

the three trans O−V−O bond angles, the magnitudes of the distortion (Δ_d) were calculated to be 1.404 and 1.442 for V1 and V2, respectively, which are comparable to those in A_2VSeO_6 (A = K, Cs).[7] Both Se atoms are three-coordinated by three O atoms in a distorted ψ-SeO_3 tetrahedral geometry, with the fourth site occupied by the lone-pair electrons, which is very common in metal selenites. The Se−O distances fall in the range of 1.670(5)−1.745(5) Å. Bond valence sum (BVS) calculations gave total bond valences of 3.99, 3.89, 4.66, and 4.85 for Se1, Se2, V1, and V2, respectively, indicating an oxidation state of 4+ for Se atoms and 5+ for V atoms.[21] Some elongated Pb−O bonds [2.849(5), 2.878(5), and 2.791(5) Å for Pb1; 2.836(5), 3.030(5), and 3.167(5) Å for Pb2] that resulted from the repulsion of the lone-pair electrons with some O atoms should be included in the calculations. With these longer Pb−O bonds considered, the calculated total bond valences of Pb1 and Pb2 are 2.04 and 1.92, respectively, indicating an oxidation state of 2+ for Pb atoms.

The two SeO_3^{2-} groups display two different coordinated modes (Scheme S2a,b in the Supporting Information). The $Se1O_3^{2-}$ anion is pentadentate: one O atom connects with two Pb atoms, the other one connects with one Pb and one V atoms, and the third one only connects with one Pb atom (Scheme S2a in the Supporting Information). The $Se2O_3^{2-}$ anion is also pentadentate: one O atom (O4) bridges with two V^{5+} and one Pb^{II} ions, and the other two O atoms are unidentate and bridge with a V or a Pb atom (Scheme S2b in the Supporting Information).

A pair of $V1^VO_6$ octahedra and a pair of $V2^VO_6$ octahedra are interconnected by edge sharing (O4···O11 and O8···O11) in a cyclic $[V_4O_{16}]^{12-}$ tetranuclear cluster unit. The V···V separations between a pair of edge-sharing VO_6 octahedra are in the range of 3.056(1)−3.271(1) Å. O11 is a μ_3 metal linker and bridges with three V centers (two V1 and one V2). It should be noted that such cyclic V_4 clusters have been observed in a number of vanadium(V) coordination compounds.[22]

The $[V_4O_{16}]^{12-}$ tetranuclear cluster units are further interconnected by $Se2O_3^{2-}$ groups via corner sharing in a 1D chain of $[V_2O_5(SeO_3)_2]^{4-}$ anions along the *b* axis (Figure 1a); the $Se1O_3^{2-}$ groups are hanging on both sides of the chain. Such neighboring chains are further bridged by Pb^{II} ions in a 3D network (Figure 1b).

When the reaction temperature was increased to 230 °C, **2**, with a different 3D inorganic skeleton, is isolated. The structure of **2** features a 3D anionic framework of $[V_3Se_5O_{18}]^{4-}$, with the Pb^{II} cations located at the 8-MR tunnels along the *b* axis (Figure 2). There are two Pb^{II} ions (both located on the mirror plane), two V^{4+} ions and two oxo anions (one at a mirror plane and one at a general site), and three selenite anions (two at the general sites and one at a mirror plane) in the asymmetric unit of **2**; hence, **2** can be also formulated as $Pb_2(V^{IV}O)_3(SeO_3)_5$.

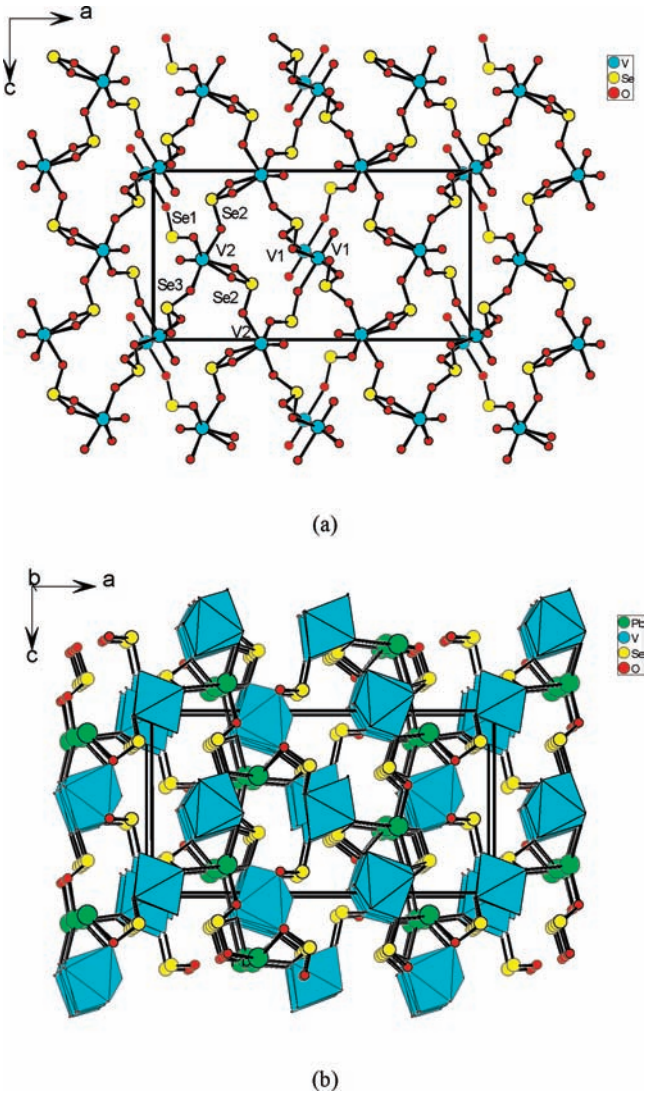

Figure 2. 3D anionic structure of $\{V_3Se_5O_{18}\}^{4-}$ (a) and view of the structure of **2** along the *b* axis (b). VO_6 octahedra are shaded in cyan. Pb, Se, and O atoms are represented by green, yellow, and red circles, respectively.

It should be pointed out that V atoms are in an oxidation state of 4+.

When only normal Pb−O bonds are considered, the Pb^{2+} ions display two different types of coordination modes. The Pb1 ion is six-coordinated by six selenite anions in a unidentate fashion, and the Pb(2) ion is four-coordinated by four selenite anions in a unidentate fashion (Scheme S1c,d in the Supporting Information). The Pb−O distances range from 2.474(3) to 2.646(3) Å. The coordination geometry around Pb1 can be described as a severely distorted octahedron because of the presence of the lone pair of the Pb^{II} ion, whereas that of Pb2 can be described as a ψ-PbO_4 square pyramid, with the pyramidal site occupied by the lone pair of the Pb^{II} ion.

V1 is octahedrally coordinated by six O atoms from five selenite anions in a unidentate fashion and an O^{2-} anion, whereas V2 is octahedrally coordinated by one selenite anion in a bidentate chelating fashion and three selenite anions in a unidentate fashion as well as an O^{2-} anion. Both V^{IV} cations are distorted toward a corner (O9 and O10 for V1 and V2, respectively; local C_4 direction) with

(21) (a) Brown, I. D.; Altermat, D. *Acta Crystallogr.* **1985**, *B41*, 244. (b) Brese, N. E.; O'Keeffe, M. *Acta Crystallogr.* **1991**, *B47*, 192.

(22) (a) Manos, M. J.; Tasiopoulos, A. J.; Tolis, E. J.; Lalioti, N.; Woolins, J. D.; Slawin, A. M. Z.; Sigalas, M. P.; Kabanos, T. A. *Chem.—Eur. J.* **2003**, *9*, 695. (b) Jiang, F.-L.; Anderson, O. P.; Miller, S. M.; Chen, J.; Mahroof-Tahir, M.; Crans, D. C. *Inorg. Chem.* **1998**, *37*, 5439. (c) Chang, Y.-D.; Chen, Q.; Khan, M. I.; Salta, J.; Zubieta, J. *Chem. Commun.* **1993**, 1872. (d) Tidmarsh, I. S.; Scales, E.; Brearley, P. R.; Wolowska, J.; Sorace, L.; Caneschi, A.; Laye, R. H.; McInnes, E. J. L. *Inorg. Chem.* **2007**, *46*, 9743.

one short [1.590(3)−1.595(4) Å], four normal [1.958(3)−2.100(3) Å], and one long [2.089(5)−2.256(3) Å] V−O bonds (Table 2), such a type of distortion has also been reported in $VO(SeO_3)\cdot H_2O$, $Cu(VO)(SeO_3)_2$, and mixed-valence KV_2SeO_7.[23] The O−V−O bond angles fall in the range of 77.5(2)−174.6(2)°. Taking into account the six V−O bond lengths as well as deviations from 180° of the three trans O−V−O bond angles, the magnitude of the distortion (Δ_d) was calculated to be 0.541 and 0.897 for V1 and V2, respectively.

The three Se^{IV} cations are in a distorted ψ-SeO_3 tetrahedral geometry, with the fourth site occupied by the lone-pair electrons as usual. The Se−O distances fall in the range of 1.640(5)−1.715(3) Å. They adopt three different coordination modes (Scheme S2c−e in the Supporting Information). The $Se1O_3$ group is tridentate, with each O atom bridged with a V^{IV} cation (Scheme S2c in the Supporting Information). The $Se2O_3$ group is pentadentate; it is connected with three V^{IV} cations and two Pb^{II} atoms. Two O atoms are bidentate, and each bridges with a Pb and a V atom, whereas the third O atom only connects with a V^{4+} center (Scheme S2d in the Supporting Information). The $Se3O_3^{2-}$ anion is hexadentate; it forms a five-membered chelating ring with one V^{IV} ion and also bridges to another V^{IV} ion and three Pb atoms (Scheme S2e in the Supporting Information). The results of BVS calculations indicate that all V and Se atoms are in an oxidation state of 4+. The calculated total bond valences are 4.05, 4.07, 4.24, 3.97, and 3.94, respectively for V1, V2, Se1, Se2, and Se3,[21] similar to that in compound **1**. With the inclusion of several elongated Pb−O bonds [2.923(3) and 2.923(3) Å for Pb1; 2.829(3), 3.071(3), and 3.151(3) Å for Pb2], the calculated total bond valences of 1.98 for Pb1 and 1.72 for Pb2, respectively, are close to the expected value of +2.0.

The VO_6 octahedra are bridged by SeO_3 groups via corner sharing in a 3D anionic framework with two types of 1D 8-MR tunnels along the *b* axis (Figure 2a). The V···V separations fall in the range of 5.416(1)−6.159(1) Å. Half of the tunnels are vacant, whereas the other half are filled by Pb^{II} ions (Figure 2b).

The structure of **3** features novel niobium(V) oxyselenite chains of $Nb_2O_3(SeO_3)_4^{4-}$ that are bridged by Pb^{2+} cations in a 3D network. The asymmetric unit of **3** consists one Pb^{II} cation, one Nb^{V} cation, two selenite anions, and two oxo anions (one at a general site and the other with the symmetry of a 2-fold axis). When only the normal Pb−O bonds are considered, the Pb^{II} cation is five-coordinated by five selenite anions in a unidentate fashion; its coordination geometry can be described as a severely distorted ψ-PbO_5 octahedron, with one vertex being occupied by the lone pair (Scheme S1e in the Supporting Information). The Pb−O distances range from 2.393(8) to 2.639(8) Å. The Nb^{V} cation is in a slightly distorted octahedral geometry, being coordinated by three selenite anions in a unidentate fashion and three O^{2-} anions. The Nb−O distances range from 1.776(7) to 2.207(7) Å. The O−Nb−O bond angles fall in the range of 81.5(3)-174.2(4)°. Taking into account the six Nb−O bond lengths as well as deviations from 180° of the three trans O−Nb−O bond angles, the magnitude of the distortion (Δ_d) was calculated to be 0.632 for Nb1. Both Se^{IV} cations are three-coordinated by three O atoms in a distorted ψ-SeO_3 tetrahedral geometry, with the fourth site occupied by the lone-pair electrons, which are similar to those in **1** and **2**. The Se−O distances fall in the range of 1.653(8)−1.730(7) Å. BVS calculations gave total bond valences of 3.99, 3.89, and 5.11 for Se1, Se2, and Nb1, respectively, indicating oxidation states of 4+ and 5+ for Se and Nb, respectively.[21] With the inclusion of a few longer Pb−O bonds [2.768(8), 2.992(8), and 3.032(8) Å], the calculated total bond valence for Pb1 is 2.00.

The two SeO_3^{2-} groups display two different coordinated modes (Scheme S2f,g in the Supporting Information). The $Se1O_3^{2-}$ anion acts as a pentadentate metal linker; two O atoms (O1 and O2) are bidentate and each is connected with two Pb atoms, whereas the third one is bonded to a Nb atom (Scheme S2f in the Supporting Information). The $Se2O_3^{2-}$ anion is tridentate; it bridges with two Nb atoms using two O atoms and one Pb atom and the third O atom (Scheme S2g in the Supporting Information).

The NbO_6 octahedra are interconnected via corner sharing (O7 and O8) in a double chain along the *c* axis; $Se2O_3$ and $Se1O_3$ groups are grafted into the chain in a bidentate bridging and a unidentate fashion, respectively (Figure 3a). The Pb^{II} ions are bridged by $Se1O_3$ groups in a 2D layer parallel to the *bc* plane (Figure 3b). The above two types of building units are further interconnected via Pb−O−Se−O−Nb bridges in a complicated 3D network with 1D tunnels of 8-MR along the *c* axis (Figure 3c). The size of the tunnel is estimated to be about 5.65 × 1.47 $Å^2$ (after deduction of the van der Waals radii of the ring atoms), and the lone pairs of the Se2 atoms are oriented toward the center of the tunnel.

The structure of **4** features a 3D network composed of a 2D layer of $[Bi_2(SeO_3)_2]^{2+}$ and 1D $[(VO_2)_2(SeO_3)_2]^{2-}$ chains. Its asymmetric unit contains two Pb^{II}, two VO_2^{+}, and four selenite anions; hence, **4** can also be formulated as $Bi_2(V^{V}O_2)_2(SeO_3)_4$. Both Bi^{3+} ions are seven-coordinated with irregular coordination geometry (Scheme S1f,g in the Supporting Information). Bi1 is coordinated by one selenite anion in a bidentate chelating fashion and five selenite anions in a unidentate fashion. The Bi−O distances fall in the range of 2.204(6)−2.715(6) Å. Both V1 and V2 are octahedrally coordinated by three selenite anions in a unidentate fashion and three O^{2-} anions. Both VO_6 octahedra are distorted toward an edge (local C_2 direction), each exhibiting two short [1.633(6)−1.666(5) Å], two normal [1.947(5)−1.982(5) Å], and two long [2.127(5)−2.347(6) Å] V−O bonds. The O−V−O bond angles fall in the range of 72.8(2)−168.5(2)°. Taking into account the six V−O bond lengths as well as the deviations from 180° of the three trans O−V−O bond angles, the magnitude of the distortion (Δ_d) was calculated to be 1.288 and 1.195 Å for V1 and V2, respectively. All four Se^{IV} atoms are three-coordinated by three O atoms in a distorted ψ-SeO_3 tetrahedral geometry, with the fourth site occupied by the lone-pair electrons. The Se−O distances fall in the range of 1.655(6)−1.750(5) Å. BVS calculations gave total bond valences of 2.82, 2.81,

(23) (a) Millet, P.; Enjalbert, R.; Galy, J. *J. Solid State Chem.* **1999**, *147*, 296. (b) Lee, K.-S.; Kwon, Y.-U.; Namgung, H.; Kim, S.-H. *Inorg. Chem.* **1995**, *34*, 4178. (c) Huan, G.-H.; Johnson, J. W.; Jacobson, A. J.; Goshorn, D. P. *Chem. Mater.* **1991**, *3*, 539.

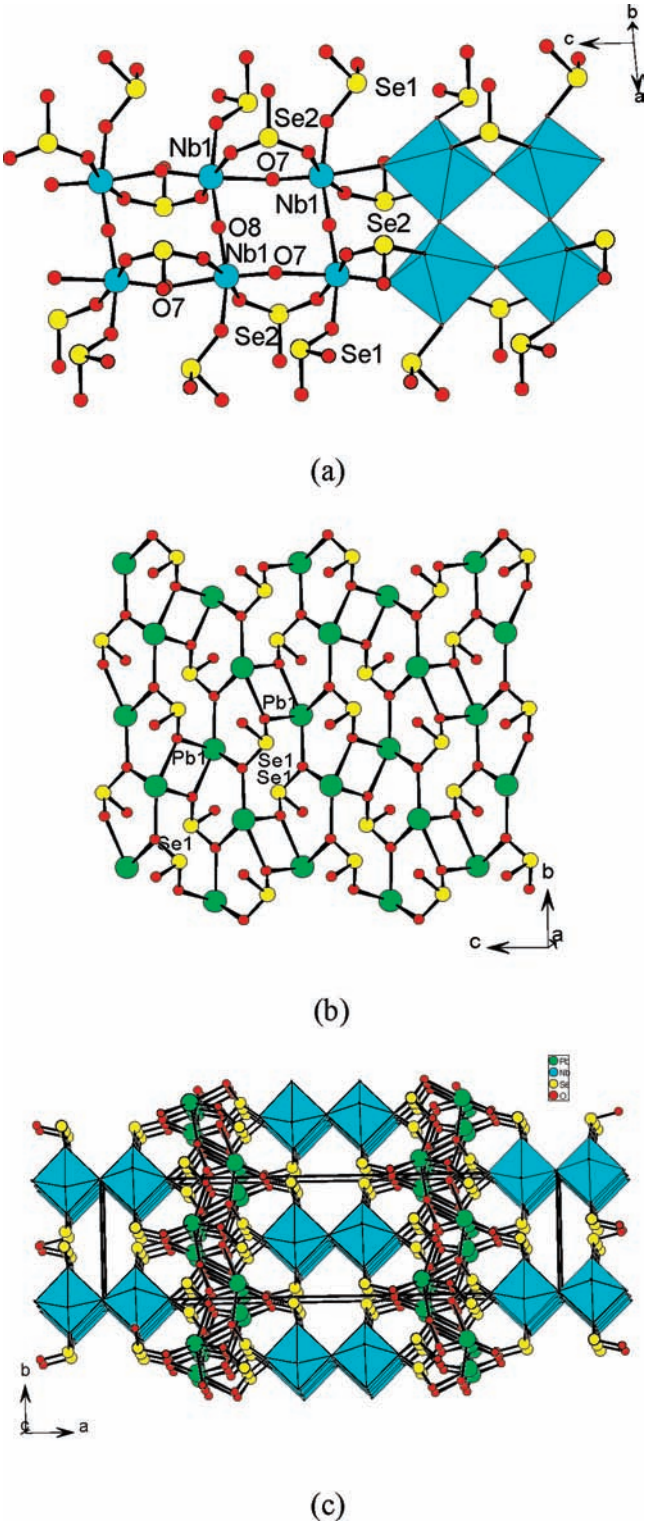

Figure 3. 1D chain of $Nb_2O_3(SeO_3)_4^{4-}$ anions (a), a lead(II) selenite layer parallel to the *bc* plane (b), and view of the structure of **3** along the *c* axis (c). NbO_6 octahedra are shaded in cyan. Pb, Se, and O atoms are represented by blue, yellow, and red circles, respectively.

3.93, 4.04, 4.05, 3.90, 4.68, and 4.71 respectively for Bi1, Bi2, Se1, Se2, Se3, Se4, V1, and V2, indicating an oxidation state of 3+ for Bi atoms, 4+ for Se atoms, and 5+ for V atoms.[21]

The four SeO_3^{2-} groups display four different coordinated modes (Scheme S2h−k in the Supporting Information).

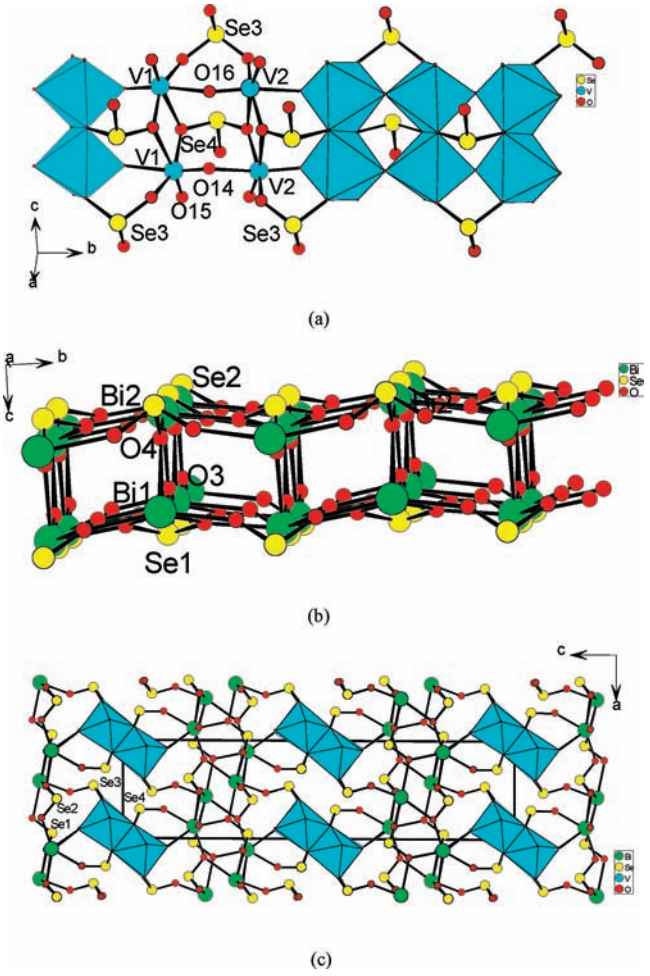

Figure 4. 1D double chain of $[(VO_2)_2(SeO_3)_2]^{2-}$ anions (a) and a double layer of $[Bi_2(SeO_3)_2]^{2+}$ (b) and view of the structure of **4** along the *c* axis (c). VO_6 octahedra are shaded in cyan. Bi, Se, and O atoms are represented by green, yellow, and red circles, respectively.

The $Se1O_3^{2-}$ anion is hexadentate; it forms a bidentate chelation with one Bi^{3+} ion and also bridges with four other Bi^{3+} ions; all three O atoms are bidentate (Scheme S2h in the Supporting Information). The $Se2O_3^{2-}$ anion is pentadentate and bridges with five Bi^{3+} ions; two O atoms are bidentate bridging, whereas the third one is unidentate (Scheme S2i in the Supporting Information). The $Se3O_3^{2-}$ anion is tridentate and bridges with one Bi and two V atoms; all three O atoms are unidentate (Scheme S2j in the Supporting Information). The $Se4O_3^{2-}$ anion also is pentadentate and bridges with four V^{5+} and one Bi^{3+} cations; O10 and O11 are bidentate bridging, whereas O12 is unidentate (Scheme S2k in the Supporting Information).

The VO_6 octahedra are interconnected through the corner sharing of oxo anions (O14 and O16) in a 1D chain, and a pair of such chains are further interconnected through edge sharing (O10 and O11) in a double chain along the *b* axis; $Se3O_3$ and $Se4O_3$ groups are grafted into the double chain in a bidentate bridging fashion (Figure 4a). The V···V distances of two edge-sharing octahedra are 3.462(1) and 3.490(1) Å, respectively, whereas those of corner-sharing ones are 3.470(1) and 3.719(1) Å, respectively, for V1−O14−V2 and V1−O16−V2 bridges. The Bi^{III} ions are bridged by $Se1O_3$ and $Se2O_3$ groups in a double layer with 1D 4-MR tunnels along the *a* axis

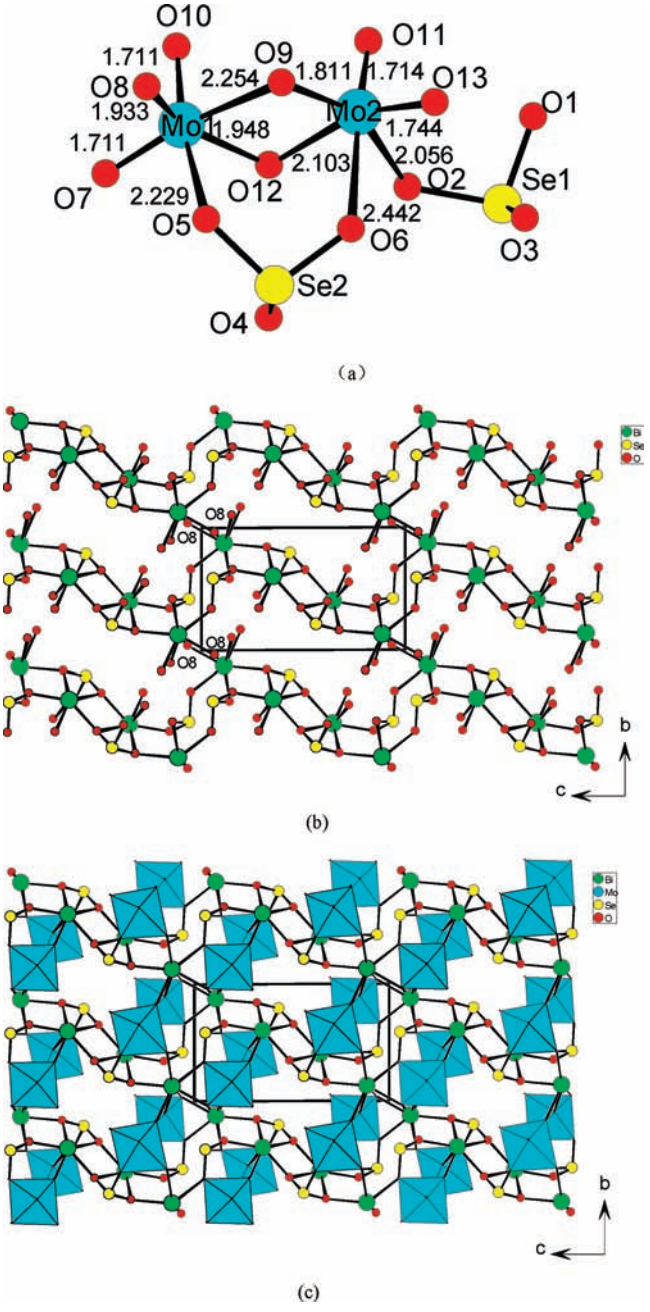

Figure 5. Dinuclear $Mo_2O_7(SeO_3)_2$ unit (a), a 3D bismuth selenite network containing 10-MR tunnels (b), and view of the structure of **5** along the *a* axis (c). MoO_6 octahedra are shaded in cyan. Bi, Se, and O atoms are represented by green, yellow, and red circles, respectively.

(Figure 4b). The above two building units are further interconnected via Bi−O−Se3−O−V bridges in a 3D architecture with narrow-long-shaped 10-MR tunnels along the *b* axis (Figure 4c).

5 is isostructural to $Nd_2W_2Te_2O_{13}$, which we reported previously.[9] The structure of **5** features a 3D network of 3D bismuth selenite, with the 10-MR tunnels along the *a* axis occupied by Mo_2O_{10} clusters (Figure 5). The asymmetric unit of $Bi_2Mo_2Se_2O_{13}$ contains two Mo, two Bi, and two Se atoms. Mo1 is octahedrally coordinated by two bridging and three terminal oxo anions as well as a selenite anion in a unidentate fashion, whereas Mo2 is octahedrally coordinated by two selenite O atoms from two selenite group anions and two terminal and two bridging oxo anions (Figure 5a). The Mo−O distances range from 1.711(5) to 2.444(5) Å, and the O−Mo−O bond angles fall in the range of 72.01(15)−170.51(19)°. Mo1 is distorted toward an edge (local C_2 direction), exhibiting two "short", two "long", and two "normal" Mo−O bonds, whereas Mo2 is displaced toward a face (local C_3 direction) with three "short" and three "long" Mo−O bonds (Table 2). Taking into account the six Mo−O bond lengths as well as the deviations of the three trans O−Mo−O bond angels from 180°, the magnitudes of the distortions (Δ_d) were calculated to be 1.13 and 1.39 Å, respectively, for Mo1 and Mo2. Bi1 and Bi2 are seven-coordinated with seven O atoms in an irregular BiO_7 polyhedron because of the presence of the lone pair of the Bi^{III} cation (Scheme S1h,i in the Supporting Information). The Bi−O distances range from 2.253(4) to 2.678(5) Å. Both Se^{IV} cations are coordinated by three O atoms in a distorted ψ-SeO_3 tetrahedral geometry, with the fourth site occupied by the lone-pair electrons. The Se−O distances fall in the range of 1.677(5)−1.748(4) Å. The selenite groups adopt two types of coordination modes (Scheme S2l,m in the Supporting Information). The $Se1O_3$ group forms a bidentate chelation with a Bi^{III} ion and also bridges with three Bi^{III} ions and one Mo^{VI} cation (Scheme S2l in the Supporting Information), whereas the $Se2O_3$ group connects with three Bi and two Mo centers (Scheme S2m in the Supporting Information). The results of BVS calculations indicate that all Bi atoms are in a 3+ oxidation state, Se atoms are in a 4+ oxidation state, and Mo atoms are in a +6 oxidation state. The calculated total bond valences for Bi1, Bi2, Se1, Se2, Mo1, and Mo2 are 2.85, 2.99, 4.01, 3.87, 6.02, and 6.03, respectively.[21]

The MoO_6 octahedra are edge-sharing in a $[Mo_2O_7(SeO_3)_2]^{4-}$ dinuclear cluster unit (Figure 5a). The BiO_7 polyhedra are bridging selenite and oxo anions in a 3D network with larger 10-MR tunnels along the *a* axis (Figure 5b). The big tunnels of bismuth selenite are based on 10-MRs composed of two $Se1O_3$ groups, two $Se2O_3$ groups, and two $Bi2O_7$ and four $Bi1O_7$ polyhedra. Mo_2 dimers are located in the above 10-MR tunnels, resulting in a 3D network of $Bi_2Mo_2Se_2O_{13}$ with much smaller voids (Figure 5c). It should be noted that, $in_2Mo_2Se_2O_{13}(H_2O)$ with an additional aqua ligand, a completely different 3D structure is displayed; it features a pillared-layered architecture composed of 2D indium(III) selenite layers that are interconnected by Mo_2O_{10} dimers, forming of 8-MR tunnels along the *b* axis.[8]

It is interesting to compare the anionic V(Nb, Mo)−Se−O substructures in compounds **1**−**5**. They feature three types of 1D chains, one dimer, and one 3D network. The $[Mo_2O_7(SeO_3)_2]^{4-}$ dinuclear cluster unit in **5** is based on two edge-sharing MoO_6 octahedra. The anionic structures of **1**, **3**, and **4** are 1D. The 1D $[V_2O_5(SeO_3)_2]^{4-}$ chain in **1** is based on tetranuclear cyclic V_4 clusters that are bridged by the selenite anions, the 1D double chain of $Nb_2O_3(SeO_3)_4^{4-}$ anions in **3** is based on corner-sharing NbO_6 octahedra, and the 1D double chain of $[(VO_2)_2(SeO_3)_2]^{2-}$ anions in **4** is based on VO_6 octahedra that are interconnected via both edge and corner sharing. There is no direct interconnection between neighboring VO_6 octahedra in the 3D anionic framework of $[V_3Se_5O_{18}]^{4-}$ in **2**, but they are bridged through selenite anions (only by V−O−Se−O−V bridges).

Optical Properties and TGA Studies. IR studies indicate that all five compounds show little absorption in the

range of 4000−1000 cm^{-1} (Figure S2 in the Supporting Information). The IR absorption bands at 910 and 886 cm^{-1} for **1**, 985, 970, 949, and 896 cm^{-1} for **2**, and 920 and 870 cm^{-1} for **4** are due to ν(V=O) or ν(V−O−V) vibrations. The absorption bands at 820, 784, 684, 661, 607, 555, 516, 500, and 439 cm^{-1} for **1**, 811, 754, 711, 665, 575, 535, and 510 cm^{-1} for **2**, and 856, 786, 702, 667, 642, 591, 512, 486, and 472 cm^{-1} for **4** can be assigned to the vibrations of ν(V−O), ν(Se−O), ν(Se−O−Se), and ν(Se−O−V).[24] For **3**, the absorption band at 937 cm^{-1} can be assigned to ν(Nb−O), whereas those at 853, 744, 722, 620, 506, 482, 447, and 424 cm^{-1} can be assigned to ν(Se−O), ν(Se−O−Se), and ν(Se−O−Nb). For **5**, the absorption bands at 925 and 960 cm^{-1} can be assigned to ν(Mo−O), and the absorption bands at 860, 752, 665, 565, 501, and 449 cm^{-1} can be assigned to ν(Se−O), ν(O−Se−O), and ν(Se−O−Mo) vibrations.[10,13e]

TGA under a nitrogen atmosphere indicate that compounds **1**−**5** are stable up to 260, 290, 390, 330, and 350 °C, respectively (Figure S3 in the Supporting Information). The five compounds all exhibit one main step of weight loss in the temperature ranges of 260−496, 290−573, 390−770, 330−520, and 350−580 °C, respectively, for **1**−**5**. The weight loss corresponds to the liberation of SeO_2 molecules. The observed weight losses of 73.0% at 500 °C for **1**, 58.27% at 580 °C for **2**, 62.06% at 770 °C for **3**, 59.37% at 520 °C for **4**, and 23.0% at 580 °C for **5** are close to the calculated ones (74%, 57.53%, 61.61%, 59.48%, and 22.7% for **1**−**5**, respectively).

Optical reflectance spectrum measurements indicate that the band gaps of compounds **1**−**5** are approximately 2.39, 3.14, 3.15, 2.2, and 2.79 eV, respectively (Figure S4 in the Supporting Information). Hence, compounds **1**−**5** can be considered to be wide-band-gap semiconductors.

Compounds **1**−**5** display a similar weak broad emission band in the blue-green light region (370−530 nm) under excitation at 237 nm for **1**, **2**, and **4** and at 286 nm for **3** and **5** (Figure S5 in the Supporting Information). These emission bands probably originated from either ligand-to-metal or metal-to-ligand charge transfer.[10c]

Magnetic Measurements of 2. Because **2** contains a paramagnetic V^{4+} ion (d^1), its magnetic properties were studied at a field of 1000 Oe in a temperature range of 2−300 K.

The temperature dependence of the magnetic susceptibility of **2** shows a maximum at about 4.5 K (Figure S6 in the Supporting Information), which is indicative of the existence of antiferromagnetic interaction between magnetic centers.[20a] The χT value at 300 K is 1.25 $cm^3\ mol^{-1}$ K, which is very close to the expected value of 1.125 $cm^3\ mol^{-1}$ K for three isolated high-spin V^{IV} ions per formula unit.[10c,25] Upon cooling to ca. 50 K, it decreases smoothly and then drops more quickly to 1.99 $cm^3\ mol^{-1}$ K at 2 K, indicating the existence of antiferromagnetic interaction between the magnetic centers. The inverse magnetic susceptibility in the range of 120−300 K obeys the Curie−Weiss law with a negative Weiss constant θ of −19.6(3) K. It is expected that the magnetic interaction mainly occurred between the V^{4+} centers within the 3D network of vanadium(IV) selenite in which the V^{IV} centers are interconnected via solely V−O−Se−O−V bridges, with the V···V separations falling in the range of 5.377(1)−6.159(1) Å.

Theoretical Studies. To further understand the chemical bonding in the five compounds, band structure as well as DOS calculations for **1**−**5** based on the DFT method were made by using the computer code CASTEP.[17]

The calculated band structures of **1**−**5** along high-symmetry points of the first Brillouin zone are plotted in Figure S7 in the Supporting Information. As is shown in Figure S7 in the Supporting Information, the top of the valence bands (VBs) is almost flat, whereas the bottom of the conduction bands (CBs) displays a small dispersion for all five compounds. For **1**, both the lowest energy (2.55 eV) of CBs and the highest energy (0.0 eV) of VBs are located between the Q and Z. Therefore, **1** displays an indirect band gap of 2.55 eV. For **2**, both the lowest energy (1.82 eV) of CBs and the highest energy (0.0 eV) of VBs are located at the G point, revealing a direct band gap of 1.82 eV. For **3**, the lowest energy (2.61 eV) of CBs is located between the A and G points and the highest energy (0.0 eV) of VBs is located between the M and A points. Hence, it displays an indirect band gap of 2.61 eV. For **4**, the lowest energy (2.5498 eV) of CBs is located at the G point and the highest energy (0.0 eV) of VBs is located at the E point. Hence, an indirect band gap of 2.55 eV can be deduced. For **5**, the lowest energy (2.52 eV) of CBs is located at the Z point and the highest energy (0.0 eV) of VBs is located at the F point. It displays an indirect band gap of 2.52 eV (Table S1 in the Supporting Information). The calculated band gaps are somehow different from the experimental values (2.39, 3.14, 3.15, 2.2, and 2.79 eV respectively for compounds **1**−**5**). This is not surprising because it is well-known that GGA does not accurately describe the eigenvalues of the electronic states. The quantitative underestimation[26] or overestimation[27] of band gaps by the DFT calculations has also been reported in other inorganic compounds.

The bands can be assigned according to the DOS and partial DOS (PDOS), as plotted in Figure S8 in the Supporting Information. The DOS and PDOS of the five compounds are quite similar. The bands just above the Fermi level are derived from V 3d (or Mo 4d or Nb 4d), Se 4p, and O 2p states in 2.26−7.35, 1.63−4.47, 1.47−6.75, 2.49−4.6, and 2.45−7.78 eV respectively for compounds **1**−**5**. The VBs just below the Fermi level are mainly from O 2p, O 2s, Pb 5d (or Bi 5d), and V 3d (or Mo 4d or Nb 4d) states mixing with a small amount of the Se 4s, Se 4p, and Pb 6s (or Bi 6s) states in all five compounds. The states of O 2s, Se 4s, and Pb 5d (or Bi 5d) dominate the VB, ranging from −22 to −7.8 eV, whereas the VBs ranging from −7.3 eV (−7.8, 7, 6.36, and 6.35 eV for

(24) (a) Sivakumar, T.; Ok, K. M.; Halasyamani, P. S. *Inorg. Chem.* **2006**, *45*, 3602. (b) Lu, Y.; Wang, E. B.; Yuan, M.; Luan, G. Y.; Li, Y. G.; Zhang, H.; Hu, C. W.; Yao, Y. G.; Qin, Y. Y.; Chen, Y. B. *J. Chem. Soc., Dalton Trans.* **2002**, 3029. (c) Xiao, D. R.; Wang, S. T.; Wang, E. B.; Hou, Y.; Li, Y. G.; Hu, C. W.; Xu, L. *J. Solid State Chem.* **2003**, *176*, 159.

(25) Van Vleck, J. H. *The Theory of Electric and Magnetic Susceptibilities*; Oxford University Press: Oxford, U.K., 1932; pp 226−261.

(26) (a) Godby, R. W.; Schluther, M.; Sham, L. J. *Phys. Rev. B* **1987**, *36*, 6497. (b) Okoye, C. M. I. *J. Phys.: Condens. Matter* **2003**, *15*, 5945. (c) Terki, R.; Bertrand, G.; Aourag, H. *Microelectron. Eng.* **2005**, *81*, 514. (d) Jiang, H.-L.; Kong, F.; Mao, J.-G. *J. Solid State Chem.* **2007**, *180*, 1764.

(27) (a) Zhu, J.; Cheng, W.-D.; Wu, D.-S.; Zhang, H.; Gong, Y.-J.; Tong, H.-N. *J. Solid State Chem.* **2006**, *179*, 597. (b) Zhu, J.; Cheng, W.-D.; Wu, D.-S.; Zhang, H.; Gong, Y.-J.; Tong, H.-N.; Zhao, D. *Eur. J. Inorg. Chem.* **2007**, 285.

compounds **1**−**5**) to the Fermi energy are mainly composed of the states of O 2p, Se 4p, and V 3d (or Mo 4d or Nb 4d) states. When the spin splitting near the Fermi level is inspected, a small splitting is observed in $Pb_2V_3Se_5O_{18}$, which is in good agreement with the effective magnetic moment from the magnetic measurements.

Population analyses allow for a more quantitative bond analysis. The calculated bond orders of Pb−O, Se−O, and V−O bonds are 0.11−0.22, 0.29−0.44, and 0.14−0.93 e, respectively, for **1**. For **2**, the calculated bond orders of Pb−O, V−O, and Se−O bonds are 0.08−0.16, 0.32−0.47, and 0.16−0.93 e, respectively. For **3**, the calculated bond orders of Pb−O, Se−O, and Nb−O bonds are 0.12−0.16, 0.33−0.47, and 0.26−0.93 e, respectively. For **4**, the calculated bond orders of Bi−O, V−O, and Se−O bonds are 0.17−0.26, 0.33−0.50, and 0.26−0.92 e, respectively. For **5**, the calculated bond orders of Bi−O, Se−O, and Mo−O bonds are 0.11−0.26, 0.34−0.43, and 0.08−0.97 e, respectively. Hence, we can say that the Se−O and V−O (or Mo−O or Nb−O) bonds are more covalent, whereas the Pb−O (or Bi−O) bond has more ionic character.

Conclusion

In summary, the first examples of lead(II) or bismuth(III) selenites with additional d^0/d^1 transition-metal ions have been successfully prepared. It should be mentioned that the three vanadium phases are obtained by using V_2O_3 as the source of V^{IV} or V^V, which otherwise could not be prepared by using V_2O_5. Hence, choosing a suitable metal source is also very important in some special cases such as in compounds **1**, **2**, and **4**. For all five compounds, two cations with a stereochemically active lone pair and a distorted TM(d^0 or d^1) O_6 octahedron have been combined in the same compound. Unfortunately, all five compounds are structurally centrosymmetric and therefore not SHG-active; however, it cannot be ruled out that some SHG materials may be found in similar systems that contain three types of cations in an asymmetric coordination geometry. It is of interest that these five compounds display five different 3D network structures. Furthermore, these five compounds feature five types of V(Nb, Mo)−Se−O anionic structures, including a zero-dimensional dinuclear cluster, three types of 1D chains, and a novel 3D open framework. Hence, this work revealed the richness of structural chemistry for these systems. Our future work will be devoted to the syntheses, crystal structures, and optical properties of other phases in the related systems.

Acknowledgment. This work was supported by National Natural Science Foundation of China (Grants 20731006, 20825104, and 20821061), the NSF of Fujian Province (Grant E0420003), and Key Project of FJIRSM (Grant SZD09001).

Supporting Information Available: X-ray crystallographic files in CIF format, tables of selected bond distances, simulated and experimental powder XRD patterns, TGA diagrams, IR spectra, band structures, and total and partial density of states (DOS and PDOS) for compounds **1**−**5**. This material is available free of charge via the Internet at http://pubs.acs.org.